ACCSCIENCE PUBLISHING

Tumor Discovery

ORIGINAL RESEARCH ARTICLE

Computational identification of immune-suppressive gene signatures associated with tumor progression and immunotherapy resistance

Kanayo Samuel Okonji[1,2]* and Harshavardhan Anandalakshmanan[3]

[1]Department of Chemistry, Faculty of Science, Federal University Oye-Ekiti, Ekiti State, Nigeria

[2]Department of Health Sciences, University of the People, Pasadena, California, United States of America

[3]Department of Biomedical Sciences, Sri Ramachandra Institute of Higher Education and Research, Chennai, India

Abstract

The tumor microenvironment integrates immune-activating and immune-suppressive cues that critically shape cancer progression and response to immunotherapy. Here, we performed a pan-cancer *in silico* analysis of transcriptome data from The Cancer Genome Atlas to define an immune-suppressive gene signature and associated immune states linked to checkpoint activity and clinical outcome. Gene set-based scoring was used to quantify $CD8^+$ T cells, regulatory T cells, macrophage subsets, and composite checkpoint and suppressive immune signatures across tumor types. Correlation and network analyses revealed that *PDCD1*, *CTLA4*, *TIGIT*, and *LAG3* form a tightly coordinated checkpoint module strongly associated with Treg enrichment, higher suppressive immune signatures, and, notably, increased $CD8^+$ T-cell infiltration, indicating co-occurring immune activation and suppression rather than mutually exclusive states. Unsupervised clustering of immune scores identified three recurrent immune subtypes, immune-poor, intermediate, and immune-enriched/suppressed, spanning multiple cancers and capturing distinct immunological configurations. The derived suppressive signature stratified patients into high- and low-risk groups, with elevated suppressive immune signature scores associated with poorer overall survival in Kaplan–Meier analyses. Multivariable Cox regression confirmed that the suppressive signature is an independent prognostic factor after adjusting for age, sex, and tumor stage, suggesting that it encodes biological information not captured by standard clinicopathologic variables. Together, these findings define a coordinated immune-suppressive program that transcends tissue of origin and provides a tractable transcriptomic biomarker for risk stratification and rational design of combination immunotherapeutic strategies.

Keywords: Immune suppressive signature; Tumor microenvironment; Immune checkpoint; Pan cancer; Survival

***Corresponding author:**
Kanayo Samuel Okonji
(kanayosamuelokonji63@gmail.com)

Citation: Okonji KS, Anandalakshmanan H. Computational identification of immune-suppressive gene signatures associated with tumor progression and immunotherapy resistance. *Tumor Discov.* doi: 10.36922/TD026130027

Received: March 23, 2026

Revised: April 21, 2026

Accepted: May 13, 2026

Published online: June 9, 2026

1. Introduction

The tumor microenvironment (TME) plays a critical role in cancer progression, immune evasion, and response to therapy.

Tumors are not merely masses of malignant cells; they comprise a complex milieu of stromal cells, immune infiltrates, extracellular matrix components, and signaling molecules that collectively influence disease trajectory and therapeutic outcomes.[1] Immune cells within the TME can be broadly categorized into effector populations that attack tumor cells and immunosuppressive populations that facilitate tumor growth and therapy resistance.[2] Understanding the balance between these immune phenotypes is essential for improving the efficacy of immunotherapies, particularly immune checkpoint inhibitors targeting programmed cell death protein 1 (PD-1), programmed death ligand 1 (PD-L1), and cytotoxic T-lymphocyte-associated protein 4 (CTLA-4).[3]

While immune checkpoint blockade has revolutionized cancer treatment, only a subset of patients across tumor types achieve durable responses.[4] Resistance to immunotherapy often arises from intrinsic tumor factors, such as TME-mediated suppression of T cell activation, exclusion of cytotoxic lymphocytes, and recruitment of regulatory T cells (Tregs) and myeloid-derived suppressor cells (MDSCs).[5] These immunosuppressive mechanisms underscore the need for comprehensive molecular characterization of the TME to identify biomarkers that predict immunotherapy response and inform combination strategies.[6]

Beyond immune checkpoint signaling, the TME is also shaped by complex cytokine-driven inflammatory networks, stromal remodeling, extracellular matrix dynamics, and hypoxia-associated metabolic adaptations that collectively influence tumor progression and therapeutic response.[7,8] Cancer-associated fibroblasts, tumor-associated macrophages, regulatory T cells, and MDSCs contribute to immunosuppressive tissue states through secretion of cytokines such as transforming growth factor-β (TGF-β), interleukin-6 (IL-6), and interleukin-10 (IL-10), which can impair cytotoxic immune activity and reinforce immune exclusion.[9] In addition, extracellular matrix remodeling and hypoxia-driven inflammatory signaling may further restrict immune infiltration and contribute to resistance against immune checkpoint blockade.[10] These interactions highlight the TME as a dynamic immunoregulatory ecosystem rather than a purely transcriptomic landscape.

In silico analyses leveragin g large public cancer genomics datasets, such as The Cancer Genome Atlas (TCGA), provide powerful tools for dissecting the molecular landscape of tumors and their microenvironments.[11] Gene expression profiling has enabled systematic evaluation of immune regulatory signatures across diverse cancer types, yielding insights into tumor immunogenicity, immune cell infiltration, and prognostic associations.[12] Computational approaches have been widely developed to estimate immune cell composition from bulk transcriptomic data, including deconvolution-based methods such as CIBERSORT and TIMER.[13,14] While these methods provide valuable insights into immune infiltration, alternative gene set-based strategies enable the quantification of coordinated immune activity across samples, facilitating comparative analyses of immune states at a pan-cancer scale.

Prognostic gene signatures derived from immune-related expression profiles have shown value in stratifying patients based on survival outcomes and predicting therapeutic benefit.[15] For example, high expression of PD-L1 and infiltration of $CD8^+$ T cells have been associated with improved responses in melanoma and lung cancer[16], whereas elevated expression of immunosuppressive mediators such as indoleamine 2,3-dioxygenase and TGF-β correlates with poor prognosis.[17,18]

Despite these advances, the complex interplay between immune-activating and immune-suppressive elements within the TME remains incompletely understood. Multi-gene signatures encompassing both effector and suppressive components may offer superior prognostic and predictive power than single markers.[19] Furthermore, differences in immune landscapes across tumor types highlight the need for pan-cancer analyses that identify conserved and unique immune features.[20]

Recent computational studies have identified immune gene modules associated with response to checkpoint blockade and overall survival, suggesting that integrated immune signatures can inform personalized therapeutic strategies.[21,22] However, many candidate signatures lack validation across independent cohorts and fail to account for the full spectrum of immunosuppressive pathways operative in the TME. Moreover, emerging evidence suggests that metabolic and stromal factors further modulate immune responses, adding layers of regulatory complexity.[23]

To address these gaps, we conducted a comprehensive *in silico* analysis of immune regulatory gene expression across multiple cancer types using large-scale transcriptomic datasets. Our aim was to define a robust immune-suppressive signature correlated with checkpoint molecule expression, immune cell infiltration, and patient survival, providing insights into mechanisms of immune resistance and potential biomarkers for immunotherapy stratification.

2. Materials and methods

2.1. Pan-cancer transcriptomic data acquisition and preprocessing

Gene expression data and corresponding clinical annotations were obtained from the TCGA repository. Only primary tumor samples were included to ensure consistency in downstream analyses. Expression matrices were processed to retain genes with reliable expression across samples, and datasets were harmonized to enable cross-cancer comparisons. Clinical metadata, including overall survival information, were integrated with the expression data to facilitate survival analyses.

2.2. Quantification of immune activity using gene set-based scoring

To characterize the immune landscape across tumors, gene set-based scoring was employed to quantify the relative enrichment of key immune cell populations, including $CD8^+$ T cells, Tregs, M1 macrophages, and M2 macrophages. These scores were derived from transcriptomic profiles to capture coordinated immune activity within each sample. In addition to individual immune cell scores, composite metrics were constructed to represent broader immune states. The checkpoint activity score (CAS) was calculated from normalized expression of the canonical immune checkpoint genes *PDCD1*, *CTLA4*, *TIGIT*, and *LAG3*. The suppressive immune signature was constructed using genes associated with checkpoint signaling (*PDCD1*, *CTLA4*, *TIGIT*, and *LAG3*), regulatory T-cell activity (*FOXP3* and *IL2RA*), and M2 macrophage polarization (*CD163* and *MRC1*). These genes were selected based on established roles in immune suppression, T-cell exhaustion, and immunoregulatory signaling within the TME. Complete gene lists used for immune scoring are provided in Table S1.

2.3. Pan-cancer immune landscape profiling and dimensionality reduction

To investigate global patterns of immune variation across cancers, principal component analysis (PCA) was performed on the immune-related scores. This approach enabled the identification of dominant axes of variation representing immune activation and macrophage polarization states. The contribution of individual immune components to these principal axes was assessed to interpret the biological drivers of immune heterogeneity across tumor types.

2.4. Stratification of tumors into immune subtypes

Unsupervised clustering was applied to immune-related scores to classify tumors into distinct immune subtypes. This stratification enabled the identification of tumor groups with similar immune characteristics across cancer types. The resulting immune subtypes were subsequently used for comparative analyses to evaluate differences in immune activity and clinical outcomes.

2.5. Cross-cancer comparison of immune suppression

To quantify differences in immunosuppressive activity across tumor types, average checkpoint activity scores were calculated for each cancer cohort. Tumors were ranked based on these scores to identify cancers with relatively high or low levels of immune suppression. This analysis enabled a systematic comparison of immune-suppression patterns across the pan-cancer dataset.

2.6. Immune checkpoint–immune landscape association analysis

To investigate the relationship between immune checkpoints and the tumor immune environment, correlation analyses were performed between checkpoint gene expression and immune-related scores. Correlation matrices were constructed to evaluate the strength of association between checkpoint molecules and immune cell populations, as well as between checkpoint molecules and composite immune scores. These analyses provided insights into the coordinated regulation of immune activation and suppression within tumors.

2.7. Survival analysis of immune signatures and subtypes

Survival analyses were conducted to evaluate the clinical relevance of immune features. Patients were stratified into high- and low-risk groups based on composite immune scores, and Kaplan–Meier survival curves were generated to assess overall survival. In addition, survival outcomes were compared across the identified immune subtypes to determine whether distinct immune states are associated with differential prognosis.

2.8. Statistical analysis and software

All statistical analyses were performed using R software (version 4.5.2).[24] Gene set-based scoring was conducted using the GSVA package.[25] Survival analyses, including Kaplan–Meier estimation and Cox proportional hazards regression, were carried out using the survival[26] and survminer[27] packages. Correlation analyses, clustering, and principal component analysis were performed using standard R functions. Data visualization was generated using established R plotting libraries.

3. Results

3.1. Checkpoint activity correlates with immune regulatory features

Correlation analysis between immune checkpoint genes and immune-related features revealed a tightly coordinated regulatory landscape (Figure 1). Strong positive associations were observed between checkpoint molecules, particularly *TIGIT*, *CTLA4*, and *PDCD1*, and both CAS and suppressive immune signature, indicating that elevated checkpoint expression is closely linked to increased immunosuppressive signaling within the TME.

Among the evaluated checkpoints, *TIGIT* showed the strongest correlations, with high associations with CAS (r = 0.90) and the suppressive immune signature (r = 0.80), followed closely by *CTLA4* and *PDCD1*, both of which demonstrated consistently strong relationships across immune features. These checkpoint genes also displayed substantial positive correlations with Tregs (e.g., *TIGIT*: r = 0.88; *CTLA4*: r = 0.87), suggesting that checkpoint activation is strongly associated with increased abundance of immunosuppressive cell populations.

In contrast, correlations with M1 macrophages were comparatively weak across all checkpoint genes, indicating limited association with pro-inflammatory macrophage activity. M2 macrophages, however, showed moderate associations, particularly with *HAVCR2* (r = 0.76), highlighting a potential link between certain checkpoint pathways and macrophage-mediated immunosuppression. Notably, checkpoint expression was also positively correlated with $CD8^+$ T cells, with *TIGIT* and *PDCD1* both showing strong associations (r = 0.83). This simultaneous association with cytotoxic T cells and suppressive features indicates that immune activation and inhibition may co-occur within tumors rather than being mutually exclusive. Hierarchical clustering further demonstrated that checkpoint genes group together based on shared correlation patterns, reinforcing the presence of a coordinated immune regulatory program. Collectively, these findings indicate that immune checkpoint expression reflects a broader immune context characterized by concurrent activation and suppression, rather than isolated inhibitory signaling.

3.2. Checkpoint genes form a coordinated regulatory module

A tightly linked module comprising PDCD1, CTLA4, TIGIT, and LAG3 was identified within the highly interconnected regulatory structure revealed by network analysis of immune checkpoint genes (Figure 2). Strong pairwise linkages and coordinated expression patterns across tumors were demonstrated by the direct links among these checkpoint molecules.

All four checkpoint genes form a dense interaction cluster rather than separate signaling axes, indicating near-complete network connectivity. This pattern is consistent with coordinated checkpoint regulation rather than independent checkpoint activity. In line with the dominant correlation patterns observed in earlier analyses, PDCD1 and TIGIT occupy central positions among the nodes, indicating substantial interactions with several checkpoint partners. The stability of this checkpoint module is further supported by the lack of peripheral or weakly connected nodes, indicating that these genes are consistently co-regulated across the dataset. The assumption that checkpoint activation constitutes a coordinated system-level response rather than individual gene-specific effects is reinforced by this tight clustering, which is consistent with the high correlations found with both CAS and suppressive immune signature.

Overall, the network topology demonstrates how tightly integrated immune checkpoint signaling is in the TME, with *PDCD1*, *CTLA4*, *TIGIT*, and *LAG3* forming a unified regulatory unit consistent with coordinated immune regulatory activity.

3.3. Pan-cancer immune landscape analysis reveals inter-tumor variability

Principal component analysis of immune-related features revealed structured organization of the pan-cancer immune landscape along coordinated immune regulatory axes (Figure S2). The first principal component (PC1) primarily reflected variation associated with CAS, suppressive immune signature, Treg enrichment, and $CD8^+$ T-cell infiltration, indicating that immune activation and suppressive signaling co-varied across tumors rather than representing mutually exclusive states. In contrast, the second principal component (PC2) was more strongly influenced by macrophage polarization patterns, separating M1- and M2-associated immune states. M2 macrophages clustered toward the positive PC2 axis together with suppressive immune features, whereas M1 macrophages localized toward the negative PC2 axis, suggesting differential contributions of macrophage phenotypes to immune regulatory organization. Collectively, these findings demonstrate that pan-cancer immune heterogeneity is structured along integrated axes of immune activation, suppression, and macrophage-associated regulation.

Significant variation in the composition of the immune landscape was found when immune-related characteristics were compared among tumor types (Figure 3). Tumors

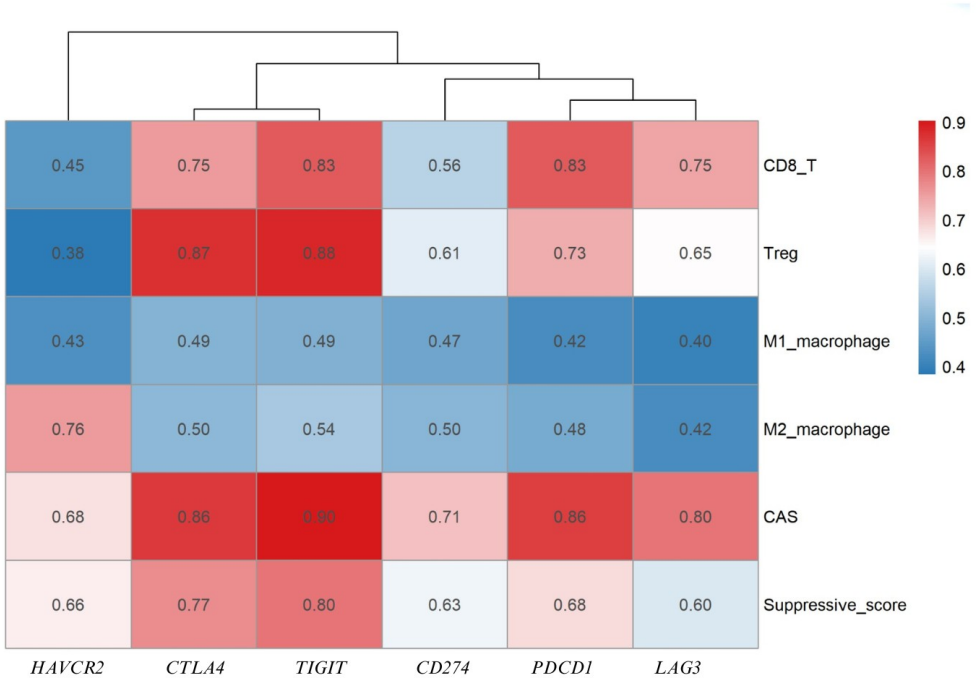

Figure 1. Correlation landscape of immune checkpoint genes and immune-related features across the pan-cancer cohort. Heatmap showing Pearson correlation coefficients between checkpoint genes (*HAVCR2*, *CTLA4*, *TIGIT*, *CD274*, *PDCD1*, and *LAG3*) and immune-related features, including $CD8^+$ T-cell infiltration, regulatory T cells (Tregs), macrophage populations, checkpoint activity score (CAS), and suppressive immune signature scores. Red indicates stronger positive correlations, whereas lighter colors indicate weaker associations. Hierarchical clustering was performed using Euclidean distance and complete linkage to identify coordinated immune regulatory patterns.

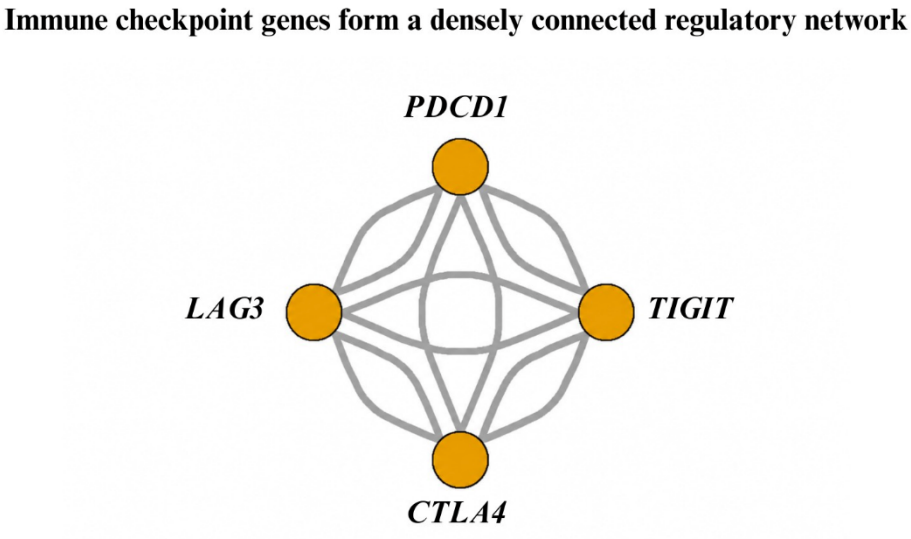

Figure 2. Network of immune checkpoint genes (*PDCD1*, *CTLA4*, *TIGIT*, *LAG3*) showing strong positive correlations across tumors. Edges represent significant Pearson correlations, indicating coordinated checkpoint regulation. Edge thickness reflects the strength of the correlation between checkpoint genes and immune-related features.

segregate according to coordinated variations in immune cell infiltration and regulatory activity, as evidenced by distinct clustering patterns.

Immune activity was consistently higher in malignancies such as cholangiocarcinoma (CHOL) and adenocortical carcinoma, as reflected by higher $CD8^+$ T cells, Tregs, and CAS scores, along with an increased suppressive immune signature. This pattern indicates that immunological activation and regulatory systems coexist within these tumors, reflecting a highly active but concurrently immunosuppressive microenvironment.

Cancers such as esophageal carcinoma (ESCA) and pancreatic adenocarcinoma (PAAD), on the other hand, showed relatively low immune enrichment across several characteristics, including decreased CD8 T cell infiltration and lower CAS values, suggesting comparatively immune-poor or less active microenvironments. Tumor types with moderate amounts of immune infiltration and regulatory activity, such as breast invasive carcinoma (BRCA), lung adenocarcinoma (LUAD), and head and neck squamous cell carcinoma (HNSC), showed intermediate patterns.

Inter-tumor variability was also influenced by macrophage polarization patterns. M2 macrophages were more strongly associated with tumors with more suppressive immune signatures, suggesting their role in creating immunosuppressive microenvironments, whereas M1 macrophage levels showed variable enrichment across malignancies.

In highly immunologically active malignancies, $CD8^+$ T cells, Tregs, CAS, and a suppressive immune signature cluster together, and hierarchical clustering showed that immune variables do not fluctuate independently but rather form coordinated patterns across tumor types. These results indicate that tumor types exhibit heterogeneous immune landscapes characterized by varying balances of immune activation and suppressive signaling, and that the tumor immune microenvironment exists along a continuum of activation and suppression.

3.4. Pan-cancer ranking of immune suppression reveals distinct tumor-specific immunological states

The composite CAS was aggregated at the cancer-type level and used to rank tumors based on their overall immune-suppressive profile, enabling comprehensive comparison of immunosuppressive activity across tumor types (Figure 4). Significant variations in immunoregulatory landscapes were highlighted by the wide range of CAS values across cancer types. The greatest average CAS was seen in adrenocortical cancer, suggesting a very immunosuppressive milieu. LUAD and HNSC were next, both showing increased CAS values, indicating checkpoint engagement and active immune modulation. Testicular germ cell tumors (TGCT), skin cutaneous melanoma, CHOL, and BRCA showed intermediate levels of immune suppression, indicating a balanced immune state with moderate checkpoint activity.

On the other hand, several tumor types showed low or negative CAS values, a marker of reduced immunosuppressive signaling. Notably, PAAD, colon adenocarcinoma (COAD), thyroid carcinoma, and ESCA all had the lowest CAS. These tumors might be indicative of immune-excluded or immunologically inactive settings with low checkpoint engagement.

Tumors such as uveal melanoma, kidney renal clear cell carcinoma (KIRC), and liver hepatocellular carcinoma showed CAS values close to zero, indicating intermediate or diverse immune responses that do not clearly fall into strongly suppressive or non-suppressive groups.

Overall, this ranking study shows that immune suppression follows a range from highly suppressive to weakly regulated microenvironments rather than being evenly distributed across malignancies. These findings emphasize the importance of tumor-specific immune profiling and suggest that the biological and clinical relevance of suppressive immune programs may differ substantially across tissue contexts, reflecting underlying heterogeneity in immune composition, stromal interactions, and checkpoint activity among cancer types.

3.5. Immune subtype stratification reveals distinct clinical and biological states

Unsupervised clustering of immune-related scores identified three major immune subtypes across the pan-cancer cohort, each characterized by distinct patterns of checkpoint activity, $CD8^+$ T-cell infiltration, and enrichment of suppressive immune signatures (Figure 5). These subtypes demonstrated clear differences in immune composition and checkpoint activity, indicating that tumors can be stratified into biologically distinct immune states. Subtype 1 was characterized by relatively low $CD8^+$ T-cell infiltration, reduced CAS, and lower suppressive immune signature scores, consistent with immune-poor or immune-desert microenvironments. Subtype 2 displayed intermediate immune activity with partial enrichment of both immune activation and suppressive features, representing a transitional immune state. In contrast, subtype 3 exhibited elevated $CD8^+$ T-cell infiltration, along with high CAS and suppressive immune signature scores, suggesting an immune-enriched but highly regulated TME characterized by simultaneous immune activation and compensatory immune suppression. Subtype 3 exhibited the highest levels of immune activity and was consistently

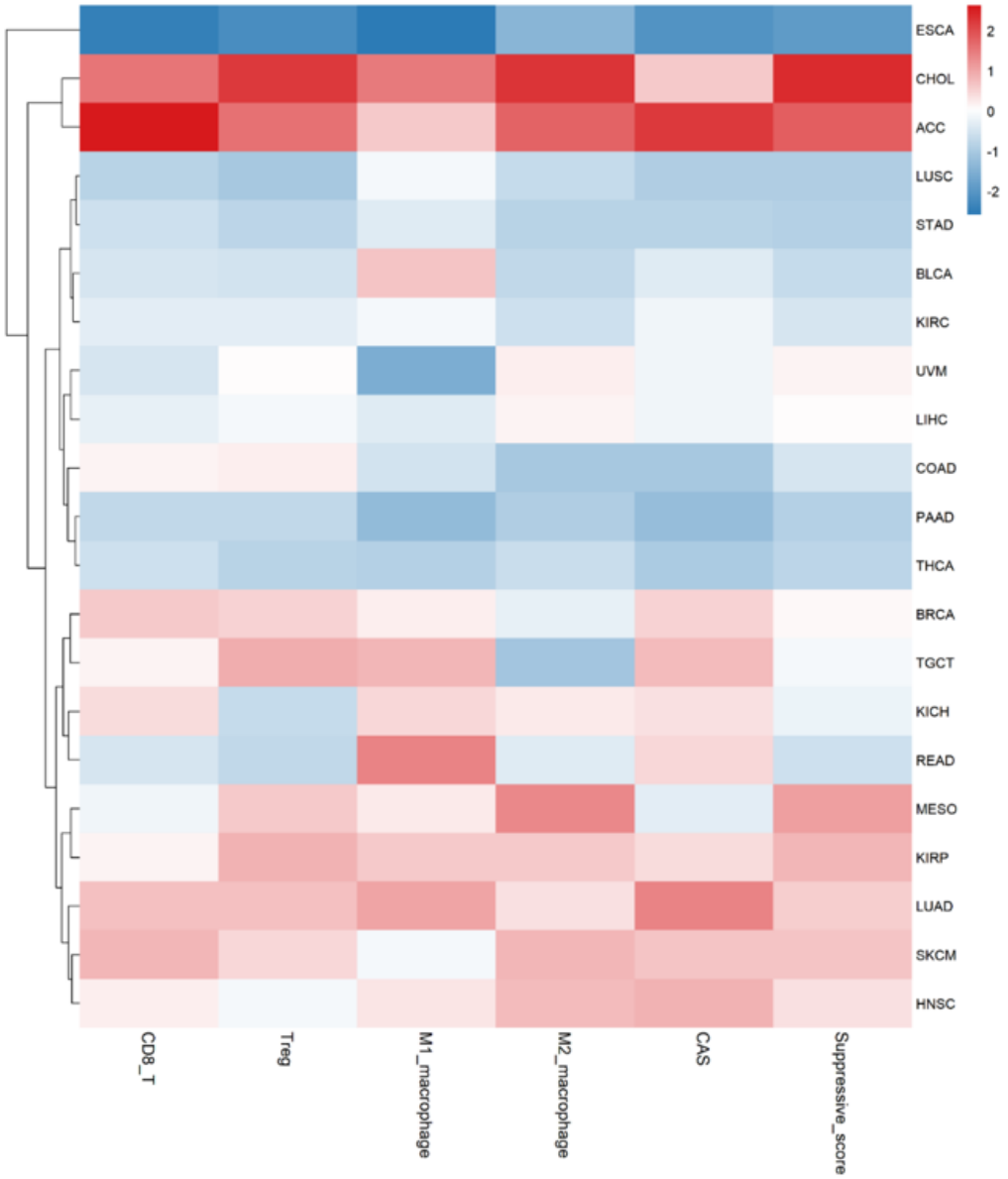

Figure 3. Heatmap of immune-related features across cancer types showing variability in CD8⁺ T cells, Tregs, macrophage populations, and composite immune scores. Distinct clustering patterns highlight heterogeneity in immune activation and suppression across tumors.
Abbreviations: CAS: Checkpoint activity score; Treg: Regulatory T cells.

characterized by elevated CD8⁺ T-cell infiltration, increased Treg abundance, higher CAS, and elevated suppressive immune signature scores across multiple cancer types. This pattern suggests an immune-enriched but highly regulated TME in which substantial immune activation coexists with strong immunosuppressive signaling. Prominent enrichment of subtype 3 was observed in LUAD, KIRC, and TGCT, consistent with the elevated CAS values observed in earlier analyses.

Subtype 2 represented an intermediate immune state characterized by moderate immune infiltration and checkpoint activity. Tumors within this subgroup displayed balanced immune profiles, suggesting partial immune activation together with moderate suppressive signaling. This subtype included cancers such as PAAD, COAD, and kidney chromophobe, which demonstrated intermediate immune patterns across the pan-cancer landscape.

In contrast, subtype 1 was characterized by relatively low immune activity, including reduced checkpoint engagement, lower Treg abundance, and decreased CD8⁺

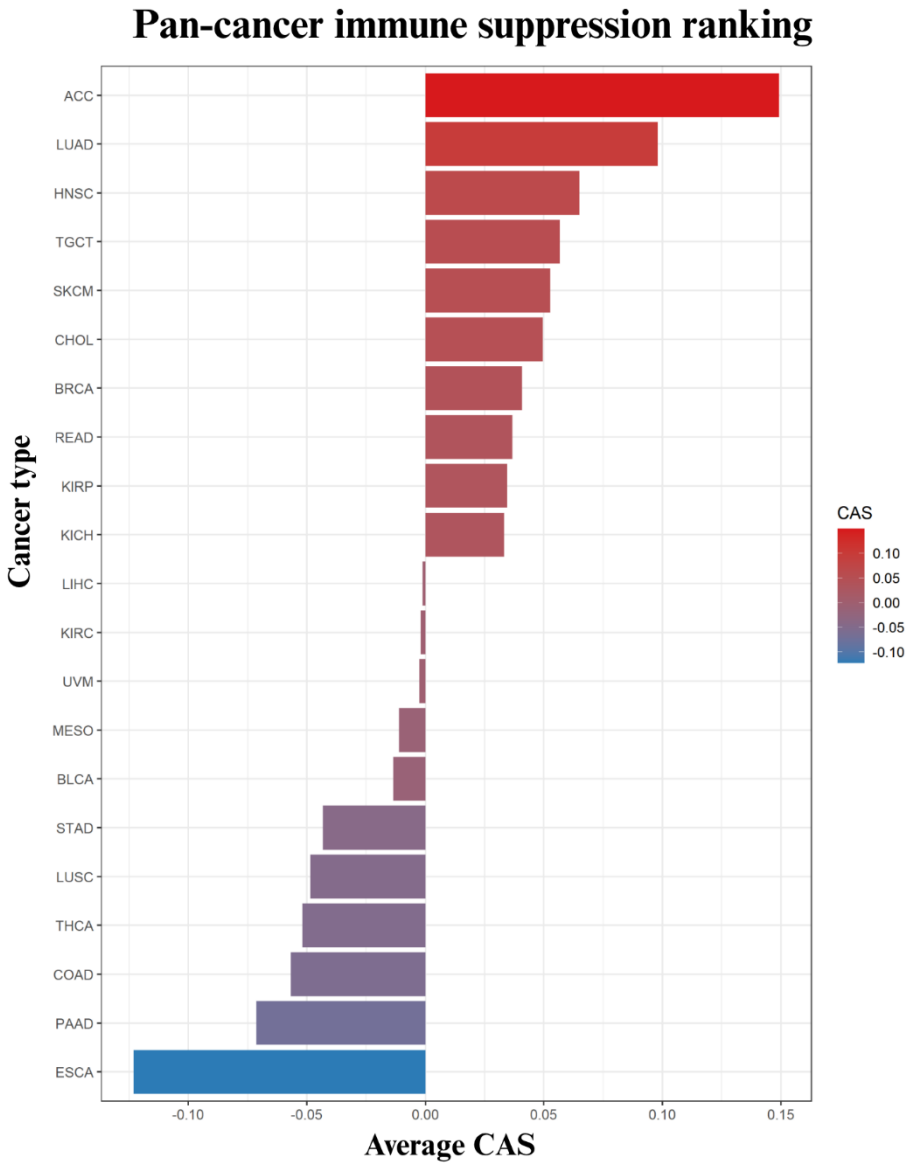

Figure 4. Bar plot showing average checkpoint activity score (CAS) across cancer types, ranked from highest to lowest. Higher CAS values indicate increased immune suppression and checkpoint engagement, whereas lower or negative values reflect reduced immunoregulatory activity.

T-cell infiltration. Lower CAS and suppressive immune signature scores suggested immune-poor or immune-excluded microenvironments. This subtype was more frequently observed in ESCA and several gastrointestinal malignancies, consistent with their comparatively lower immune activity.

Hierarchical clustering further supported the presence of conserved immune programs across tumor types, indicating that these immune subtypes reflect systematic variation in immune organization rather than random distribution patterns. Collectively, these findings demonstrate that subtype classification provides a useful framework for capturing pan-cancer immune heterogeneity and distinguishing biologically distinct immune states across malignancies.

3.6. Immune subtypes exhibit distinct survival outcomes

Kaplan–Meier survival analysis was performed for each of the three subtypes to assess the clinical significance of the identified immunological subtypes (Figure 6). Immune

stratification captures clinically significant heterogeneity in patient outcomes, as evidenced by the significant differences in overall survival between subtypes (log-rank $p = 0.0048$).

With a continuously decreased survival probability over time compared to the other groups, subtype 2 showed the worst survival outcomes. This subtype may indicate a defective immunological state in which limited immune infiltration fails to elicit effective antitumor responses. It is characterized by intermediate immune activation but insufficient cytotoxic engagement.

Over longer follow-up periods, subtype 1 showed a gradual decline in survival, although it was comparatively better during early time points. Despite lower levels of immunosuppressive signaling, this subtype's reduced immune activity suggests an immunosuppressive environment that may limit effective tumor treatment.

Subtype 3, on the other hand, showed significantly better long-term survival, especially at later time points. High immune activation, along with increased checkpoint and suppressive signaling, characterizes this subtype, indicating that tumors in this group maintain active immune engagement that may partially limit tumor growth even in the presence of regulatory systems.

Overall, these results show that immune subtypes are both physiologically unique and therapeutically significant, with varying survival rates indicating the balance between immune activation and suppression in the TME.

3.7. Suppressive immune signature is associated with poor overall survival

Kaplan–Meier survival analysis was performed after patients were divided into high- and low-signature groups based on the median signature score to assess the prognostic significance of the derived suppressive immune signature (Figure 7). The two groups' overall survival differed significantly (log-rank $p < 0.0001$), suggesting that the suppressive signature reliably captures clinically important differences in patient outcomes.

Survival was consistently lower for patients with high suppressive signature scores than for those with low levels. Early on and continuing throughout the follow-up period, there was a clear divergence between the survival curves, indicating that increased immunosuppressive activity is associated with a poor prognosis for all forms of cancer.[28]

As a result of a TME with a lower immunosuppressive burden and possibly stronger antitumor immune responses, patients with low suppressive immune signatures showed better survival prospects. The biological significance of the signature is further supported by this observation, which is consistent with the positive correlations seen between checkpoint molecule expression, regulatory immune populations, and suppressive immune signature. All of these findings demonstrate the suppressive immune signature's potential value for patient classification and treatment decision-making by establishing it as a major prognostic actor in pan-cancer analysis.

3.8. Independent prognostic significance of the suppressive immune signature

Cox proportional hazards regression was used, accounting for important clinical factors such as age, gender, and tumor stage, to determine whether the suppressive immune signature independently predicts patient survival (Figure 8).

With a hazard ratio (HR) of roughly 1.1 (95% CI: 1.0–1.1; $p < 0.001$), the suppressive immune signature remained strongly correlated with overall survival in the multivariate model. This suggests that, independent of known clinical variables, higher suppressive immune signatures are linked to a higher chance of death. The robustness of this link across the pan-cancer sample is supported by the narrow confidence interval and strong statistical significance, despite the low effect size.

Tumor stage showed the greatest influence on survival among clinical variables. Stage II (HR = 1.6), Stage III (HR ≈ 2.4), and Stage IV (HR ≈ 4.1) had increasingly greater hazard ratios than Stage I (reference), indicating a distinct stepwise increase in mortality risk with advancing disease stage. Although the effect size was small (HR = 1.0), age was also strongly correlated with survival, consistent with its role as a continuous covariate.

There were clear gender-based disparities, with male patients showing a considerably higher risk than female patients (HR = 1.4; $p < 0.001$). Crucially, the suppressive immune signature remained statistically significant after adjustment for these variables, although the observed effect size was modest, suggesting that it captures prognostic information beyond conventional clinical variables. Collectively, these findings indicate that the suppressive immune signature captures reproducible prognostic variation across the pan-cancer cohort, although its modest effect size suggests that it should be interpreted as a component of broader immune and clinical risk frameworks rather than a standalone prognostic determinant.

3.9. External validation of checkpoint-associated suppressive markers

To further evaluate the external reproducibility of the checkpoint-associated suppressive immune landscape

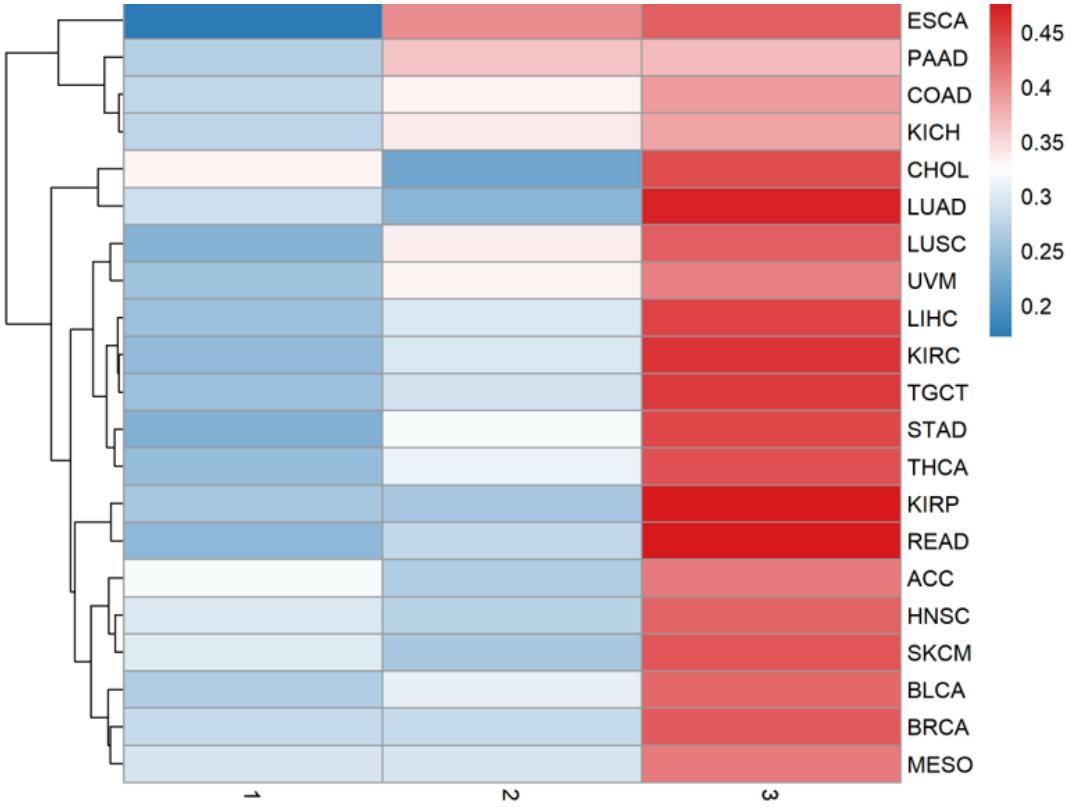

Figure 5. Pan-cancer immune subtype enrichment heatmap showing the distribution of three immune subtypes across cancer types. Samples were grouped using unsupervised hierarchical clustering based on immune-related scores. Red indicates relative enrichment, whereas blue indicates reduced enrichment. Subtype 3 exhibits high immune activation and suppression, subtype 2 represents an intermediate immune state, and subtype 1 reflects immune-poor microenvironments.

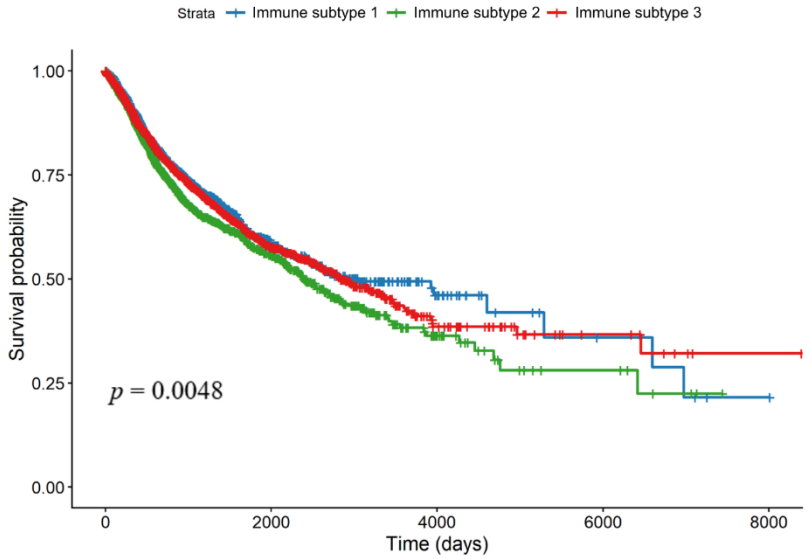

Figure 6. Kaplan–Meier survival curves showing overall survival across immune subtypes. Subtype 2 exhibits the poorest prognosis, while subtype 3 demonstrates relatively improved long-term survival (log-rank $p = 0.0048$).

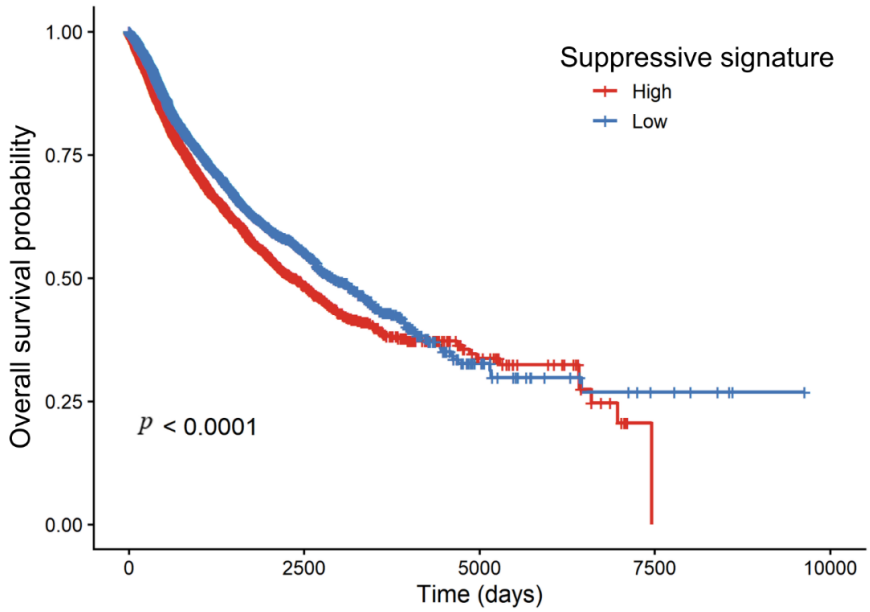

Figure 7. Kaplan–Meier survival curves comparing overall survival between high- and low-suppressive immune signature groups. Patients with high suppressive immune signatures exhibit significantly poorer survival (log-rank $p < 0.0001$). Survival differences between groups were evaluated using the log-rank test.

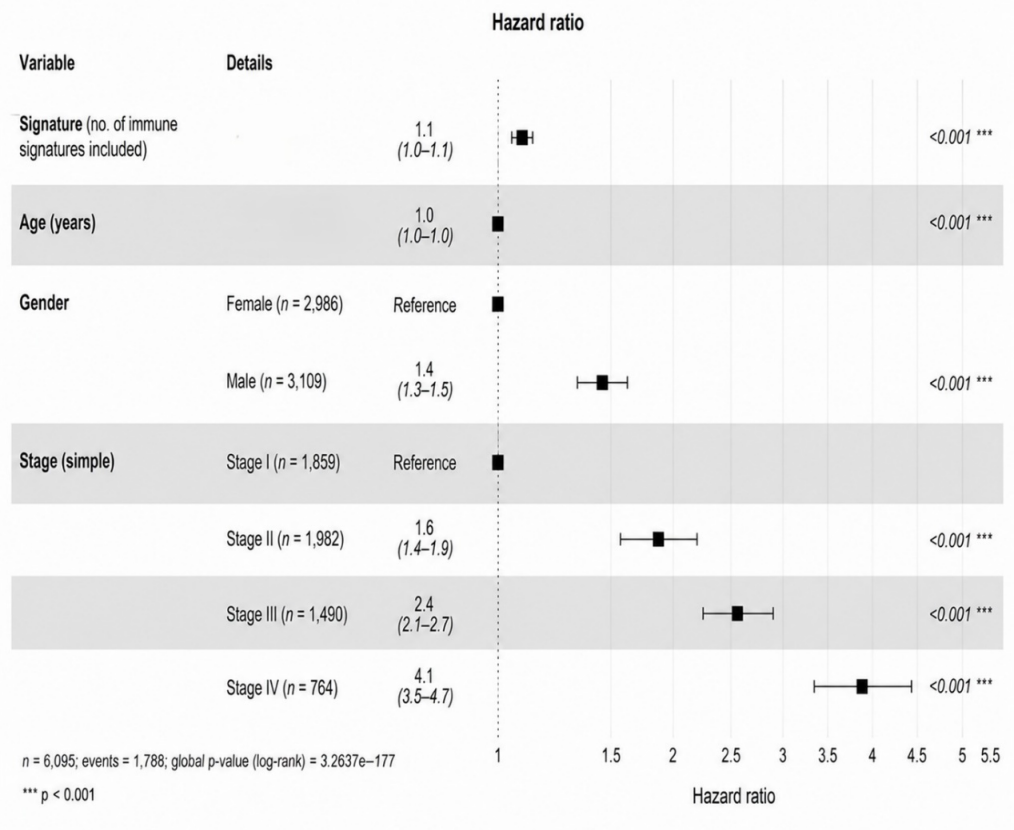

Figure 8. Forest plot of multivariate Cox proportional hazards regression analysis demonstrating the independent association of the suppressive immune signature with overall survival after adjustment for age, gender, and tumor stage. Hazard ratios (HRs) and 95% confidence intervals were estimated using multivariable Cox proportional hazards regression. *** denotes $p < 0.001$.

identified in the TCGA pan-cancer cohort, independent survival analyses were performed using publicly available datasets from the KM Plotter platform (Figure 9). Elevated expression of key checkpoint-associated genes, including *TIGIT*, *CTLA4*, *PDCD1*, and *LAG3*, was significantly associated with overall survival across independent cohorts. *TIGIT* expression showed a significant survival association (HR = 0.66, log-rank $p = 0.0074$), while *CTLA4* (HR = 0.70, $p = 0.039$), *PDCD1* (HR = 0.64, $p = 0.011$), and *LAG3* (HR = 0.68, $p = 0.024$) demonstrated similar trends. *HAVCR2* showed a comparable but non-significant survival pattern (HR = 0.80, $p = 0.19$). Collectively, these findings support the broader reproducibility of the checkpoint-associated suppressive immune program beyond the TCGA discovery cohort and suggest that the observed immune relationships are not dataset-specific artifacts. These findings likely reflect the context-dependent role of checkpoint expression, in which elevated checkpoint levels may indicate pre-existing antitumor immune infiltration rather than isolated immunosuppressive activity.

3.10. External validation of the suppressive immune signature

To evaluate the external robustness of the suppressive immune signature, validation analysis was performed using an independent LUAD cohort, GSE68465. Signature enrichment scores were calculated using ssGSEA based on the suppressive immune gene set. Patients with elevated suppressive signature scores showed a trend toward poorer overall survival than those with low scores, although the difference did not reach statistical significance (log-rank $p = 0.11$; Figure S1). These findings suggest partial preservation of suppressive immune-associated transcriptional patterns across independent cohorts while also indicating cohort- and tumor-specific variability in prognostic strength.

4. Discussion

Immunosuppressive programs provide a coordinated transcriptional axis that spans tissue of origin and captures clinically significant variability in the TME, according to our pan-cancer analysis.[20,29,30] Tightly co-expressed checkpoint receptors (*PDCD1*, *CTLA4*, *TIGIT*, *LAG3*), enrichment of Tregs and M2-like macrophage profiles, and a composite suppressive immune signature that independently correlates with poor overall survival after controlling for age, sex, and stage are characteristics of this axis.[30–32]

Tumors segregate into recurrent immune subtypes with distinct prognostic and therapeutic consequences. These subtypes range from IFN-γ-dominant and inflammatory to lymphocyte-depleted and immunologically quiet states, according to TCGA-scale immunogenomic research.[20,33] These subgroups highlight the need for pan-cancer rather than tumor-type-restricted biomarkers by showing that immune phenotypes frequently transcend histology. Our work complements these frameworks by focusing on an immunosuppressive continuum, as measured by CAS and a suppressive signature. This is in line with evidence that the balance between stimulatory and suppressive programs better predicts outcome than either program alone.[30, 34]

The idea that T-cell exhaustion has been associated with coordinated expression of checkpoint receptors rather than distinct pathways is supported by the discovery that *PDCD1*, *CTLA4*, *TIGIT*, and *LAG3* constitute a closely linked module with substantial correlations to CAS, suppressive immune signature, and Treg abundance.[35–37] Particularly, *TIGIT* is strongly expressed on intratumoral T cells and Tregs, identifies functionally exhausted populations, and has been associated with reduced survival and resistance to PD-1 treatment.[38,39] In preclinical and clinical contexts, combinatorial checkpoint inhibition can affect co-expression of PD-1 with TIGIT or LAG-3 on $CD8^+$ T cells, which has been consistently linked to dysfunctional yet tumor-reactive populations.[40–43] Our network results, which show that these checkpoints exhibit coordinated expression patterns consistent with a unified regulatory program firmly embedded within a larger suppressive transcriptional program, provide support for this theory.

We distinguish three immunological states across tumor types: immune-poor, immune-enriched but strongly repressed, and immune-intermediate. Prior TCGA immune subtype schemes, which contrast lymphocyte-depleted or immunologically quiet classes with inflammatory, IFN-γ-dominant conditions, are echoed but simplified by this stratification.[44–46] Significantly, the immune-enriched/suppressed subtype exhibits both elevated CAS suppressive immune signatures and high $CD8^+$ T-cell scores, which are consistent with "inflamed but restrained" phenotypes as defined by the tumor inflammation signature (TIS) and associated adaptive resistance programs.[20,42,47] The resultant suppressive signature, which mirrors independent pan-cancer immune gene signatures in which overexpression of particular immune-related genes and enrichment of M2 macrophages are associated with shorter overall survival, effectively divides patients into high- and low-risk groups.[29]

Multivariable Cox regression analysis demonstrated that the suppressive immune signature retained statistical significance after adjustment for age, sex, and tumor stage, indicating that it captures prognostic variation beyond conventional clinicopathologic variables.[48–50] However, the observed hazard ratio was modest (HR ≈ 1.1), suggesting that the magnitude of its independent prognostic

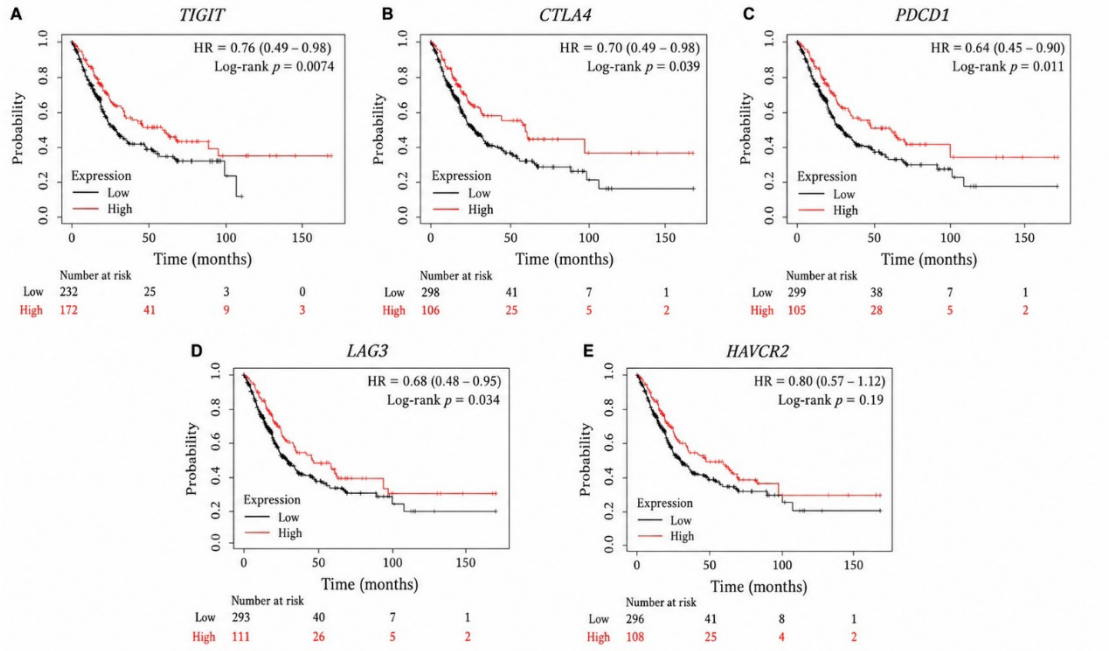

Figure 9. External validation of checkpoint-associated suppressive markers using KM Plotter datasets. Kaplan–Meier overall survival analyses for (A) *TIGIT*, (B) *CTLA4*, (C) *PDCD1*, (D) *LAG3*, and (E) *HAVCR2* expression in independent public cohorts. Patients were stratified into high (red) and low (black) expression groups based on the median cutoff. Hazard ratios (HR) with 95% confidence intervals and log-rank *p*-values are shown in each panel. Higher expression of *TIGIT*, *CTLA4*, *PDCD1*, and *LAG3* is significantly associated with improved overall survival in external cohorts, whereas *HAVCR2* shows a similar but non-significant trend.

contribution is limited. Therefore, while the suppressive immune signature appears biologically informative at the population level, its immediate clinical applicability as a standalone prognostic biomarker may be constrained. These findings instead support its potential utility within integrated immune-risk frameworks that incorporate additional molecular, clinical, and microenvironmental features. The signature is conceptually consistent with the Tumor Immune Dysfunction and Exclusion (TIDE) framework, which predicts poor survival and a lower chance of benefit from PD-1/CTLA-4 inhibition based on composite assessments of T-cell dysfunction and exclusion.[22,29] All of these lines of evidence point to the suppressive signature as a clinically meaningful and biologically consistent indicator of persistent immune evasion.

High checkpoint expression correlates with both CD8 T-cell infiltration and regulatory cell concentration, supporting the idea that immunological activation and suppression co-occur rather than defining mutually incompatible states.[51–53] This is in line with findings showing tumors that respond well to PD-1 inhibition frequently have an innate but repressed adaptive immune response, as evidenced by high TIS or comparable inflammatory scores. Experimental and early clinical data strongly support dual or multi-checkpoint blockade (e.g., PD-1 plus TIGIT or LAG-3) and rational combinations with agents targeting Tregs, MDSCs, or M2-like macrophages in such "hot-but-suppressed" tumors with high CAS and suppressive immune signatures.[34,54] As demonstrated by pancreatic ductal adenocarcinoma, where dense stroma and myeloid-dominated TMEs require stromal or myeloid-directed interventions prior to or in conjunction with checkpoint blockade, tumor types with low CAS and minimal immune infiltration most likely represent immune-excluded or inert states.[55,56]

All of these results indicate a paradigm in which immune suppression in cancer involves coordinated immune regulatory networks that integrate checkpoint signaling, regulatory immune cells, and macrophage polarization, rather than being driven by distinct processes.[57,58] Our findings offer a scalable approach for pan-cancer immunological stratification by capturing this axis through a uniform suppressive signature. It also emphasizes the significance of targeting various immunoregulatory systems to overcome entrenched immune evasion.[59]

Although PCA was used in this study due to its

interpretability and ability to capture the global variance structure, alternative nonlinear dimensionality reduction methods such as *t*-distributed stochastic neighbor embedding (*t*-SNE) have been increasingly applied to high-dimensional biological datasets. *t*-SNE is particularly effective in preserving local neighborhood structure and revealing hidden clusters in complex transcriptomic and genetic data, whereas PCA primarily preserves global variance patterns. Recent studies using biological and omics datasets have demonstrated that *t*-SNE can better resolve sample heterogeneity and uncover latent subpopulation structures compared with PCA in certain applications. In addition, benchmark studies across high-dimensional systems have shown that *t*-SNE may outperform PCA in clustering and visualization tasks depending on the data structure.[60–63]

Because this study is retrospective and relies on bulk RNA-sequencing, the spatial structure of immunological and stromal components is obscured, and cell-type resolution is limited. As has been done for TIS, TIDE, and other signatures, the predictive utility for immunotherapy response has not yet been demonstrated in independent immune checkpoint blockade-treated datasets, as most TCGA cohorts are treatment-naïve. Moreover, we did not incorporate antigenicity, mutational characteristics, or metabolic and stromal pathways that are known to influence immune escape. Because the present study is based on transcriptomic correlation analyses, the findings should be interpreted as associative rather than mechanistic. Experimental validation will be necessary to establish causal relationships between checkpoint activity, suppressive immune programs, and clinical outcomes. Furthermore, although statistically significant, the relatively modest effect sizes observed in survival analyses suggest that additional molecular and clinical variables will likely be necessary to improve predictive performance in translational settings. Future research should use single-cell and spatial profiling to analyze the suppressive signature's cellular foundations, validate it in prospective immunotherapy trials, and incorporate it into multi-omics models that account for microenvironmental, metabolic, and genomic factors contributing to immune resistance.

Although exploratory external validation in the independent LUAD cohort GSE68465 demonstrated directionally consistent survival trends, statistical significance was not achieved, suggesting that the prognostic impact of the suppressive immune signature may vary across tumor contexts and transcriptomic platforms. Several factors may contribute to this variability, including cohort heterogeneity, limitations of the microarray platform, incomplete representation of all suppressive genes (e.g., *TIGIT*), and differences in immune microenvironment composition between pan-cancer and single-cancer settings. Accordingly, the suppressive signature may more robustly reflect coordinated immune regulatory states at the systems level rather than functioning as a universally transferable prognostic classifier. Future studies involving larger, multicentre cohorts and immunotherapy-treated patients will be important for further evaluating its clinical applicability.

In addition, although the pan-cancer framework enables identification of conserved immune regulatory programs across malignancies, this approach may obscure tumor-specific immune dynamics and microenvironmental heterogeneity unique to individual cancer types. Distinct tissue contexts, stromal composition, mutational landscapes, and inflammatory states can substantially influence immune regulation and checkpoint activity. Therefore, future tumor-specific analyses may provide greater biological resolution and help refine the translational relevance of the suppressive immune signature within individual cancer settings.

5. Conclusion

This study shows that immune suppression in cancer arises as a coordinated transcriptional axis that integrates checkpoint signaling, regulatory immune cells, and macrophage polarization rather than being driven by discrete processes. Beyond standard clinical factors, this axis independently predicts adverse survival and defines conserved pan-cancer immunological states. Our work provides a robust framework for patient categorization by capturing this biology via a uniform suppressive signature. It also emphasizes the need to combine immunotherapeutic approaches that simultaneously boost effector responses and disrupt suppressive networks.

Acknowledgments

The authors appreciate the collaborative support of the Chemistry Collaborative Research Environment (CHEMCORE) for providing and enabling an academic network for interdisciplinary research discussions and technical guidance during manuscript preparation.

Funding

None.

Conflict of interest

The authors declare that they have no competing financial or non-financial interests.

Author contributions

Conceptualization: Kanayo Samuel Okonji
Data curation: Harshavardhan Anandalakshmanan & Kanayo Samuel Okonji
Formal analysis: Harshavardhan Anandalakshmanan
Methodology: Kanayo Samuel Okonji
Supervision: Kanayo Samuel Okonji
Validation: Harshavardhan Anandalakshmanan & Kanayo Samuel Okonji
Visualization: Harshavardhan Anandalakshmanan
Writing–original draft: Kanayo Samuel Okonji
Writing–review & editing: Kanayo Samuel Okonji & Harshavardhan Anandalakshmanan
All authors approved the final manuscript.

Ethics approval and consent to participate

Not applicable.

Consent for publication

Not applicable.

Availability of data

Data are available upon reasonable request to the corresponding author.

Further disclosure

The authors declare that no generative AI or AI-assisted technologies were used in the design, analysis, or preparation of this manuscript.

References

1. Hanahan D, Weinberg RA. Hallmarks of cancer: the next generation. *Cell*. 2011;144(5):646-674.
doi: 10.1016/j.cell.2011.02.013

2. Fridman WH, Pagès F, Sautès-Fridman C, Galon J. The immune contexture in human tumours: impact on clinical outcome. *Nat Rev Cancer*. 2012;12(4):298-306.
doi: 10.1038/nrc3245

3. Topalian SL, Drake CG, Pardoll DM. Immune checkpoint blockade: A common denominator Approach to Cancer Therapy. *Cancer Cell*. 2015;27(4):450-461.
doi: 10.1016/j.ccell.2015.03.001

4. Sharma P, Allison JP. The future of immune checkpoint therapy. *Science*. 2015;348(6230):56-61.
doi: 10.1126/science.aaa8172

5. Joyce JA, Fearon DT. T cell exclusion, immune privilege, and the tumor microenvironment. *Science*. 2015;348(6230):74-80.
doi: 10.1126/science.aaa6204

6. Ribas A, Wolchok JD. Cancer immunotherapy using checkpoint blockade. *Science*. 2018;359(6382):1350-1355.
doi: 10.1126/science.aar4060

7. Hu Q, Zhu Y, Mei J, Liu Y, Zhou G. Extracellular matrix dynamics in tumor immunoregulation: from tumor microenvironment to immunotherapy. *J Hematol Oncol*. 2025;18(1):65.
doi: 10.1186/s13045-025-01717-y

8. de Visser KE, Joyce JA. The evolving tumor microenvironment: From cancer initiation to metastatic outgrowth. *Cancer Cell*. 2023;41(3):374-403.
doi: 10.1016/j.ccell.2023.02.016

9. Raskov H, Orhan A, Gaggar S, Gögenur I. Cancer-Associated Fibroblasts and Tumor-Associated Macrophages in Cancer and Cancer Immunotherapy. *Front Oncol*. 2021;11:668731.
doi: 10.3389/fonc.2021.668731

10. Zhang W, Xiang Y, Lu C, *et al.* The extracellular matrix in inflammation and cancer. *Mol Biomed*. 2026;7(1):21.
doi: 10.1186/s43556-026-00415-6

11. Weinstein JN, Collisson EA, Mills GB, *et al.* The Cancer Genome Atlas Pan-Cancer analysis project. *Nat Genet*. 2013;45(10):1113–1120.
doi: 10.1038/ng.2764

12. Gentles A, Newman A, Liu C, *et al.* The prognostic landscape of genes and infiltrating immune cells across human cancers. *Nat Med*. 2015;21(8):938–945.
doi: 10.1038/nm.3909

13. Newman A, Liu C, Green M, *et al.* Robust enumeration of cell subsets from tissue expression profiles. *Nat Methods*. 2015;12(5):453–457.
doi: 10.1038/nmeth.3337

14. Li B, Severson E, Pignon JC, *et al.* Comprehensive analyses of tumor immunity: implications for cancer immunotherapy. *Genome Biol*. 2016;17(1):174.
doi: 10.1186/s13059-016-1028-7

15. Rooney MS, Shukla SA, Wu CJ, Getz G, Hacohen N. Molecular and genetic properties of tumors associated with local immune cytolytic activity. *Cell*. 2015;160(1-2):48-61.
doi: 10.1016/j.cell.2014.12.033

16. Tumeh P, Harview C, Yearley J, *et al.* PD-1 blockade induces responses by inhibiting adaptive immune resistance. *Nature*. 2014;515(7528):568–571.
doi: 10.1038/nature13954

17. Munn DH, Mellor AL. IDO in the Tumor Microenvironment: Inflammation, Counter-Regulation, and Tolerance. *Trends Immunol*. 2016;37(3):193-207.

doi: 10.1016/j.it.2016.01.002

18. Mariathasan S, Turley S, Nickles D, *et al.* TGFβ attenuates tumour response to PD-L1 blockade by contributing to exclusion of T cells. *Nature*. 2018;554(7693):544–548.

doi: 10.1038/nature25501

19. Cristescu R, Mogg R, Ayers M, *et al.* Pan-tumor genomic biomarkers for PD-1 checkpoint blockade-based immunotherapy. *Science*. 2018;362(6411):eaar3593.

doi: 10.1126/science.aar3593

20. Thorsson V, Gibbs DL, Brown SD, *et al.* The Immune Landscape of Cancer. *Immunity*. 2018;48(4):812-830.e14.

doi: 10.1016/j.immuni.2018.03.023

21. Ayers M, Lunceford J, Nebozhyn M, *et al.* IFN-γ-related mRNA profile predicts clinical response to PD-1 blockade. *J Clin Invest*. 2017;127(8):2930-2940.

doi: 10.1172/JCI91190

22. Jiang P, Gu S, Pan D, *et al.* Signatures of T cell dysfunction and exclusion predict cancer immunotherapy response. *Nat Med*. 2018;24(10):1550–1558.

doi: 10.1038/s41591-018-0136-1

23. Li S, Zhang Y, Tong H, *et al.* Metabolic regulation of immunity in the tumor microenvironment. *Cell Rep*. 2025;44(11):116463.

doi: 10.1016/j.celrep.2025.116463

24. R Core Team. *R:* A language and environment for statistical computing. R Foundation for Statistical Computing. 2025. https://www.r-project.org/.

25.Hänzelmann S, Castelo R, Guinney J. GSVA: Gene set variation analysis for microarray and RNA-seq data. *BMC Bioinform.* 2013;14(1):7.

doi: 10.1186/1471-2105-14-7

26. Terry M. Therneau. *A package for survival analysis in R (Version* 3.8-3). 2024. Available from: https://CRAN.R-project.org/package=survival.

27. Alboukadel Kassambara, Marcin Kosinski, Przemyslaw Biecek. *survminer: Drawing survival curves using ggplot2* (Version 0.5.2). 2026.

doi: 10.32614/CRAN.package.survminer

28. Lánczky A, Győrffy B. Web-Based Survival Analysis Tool Tailored for Medical Research (KMplot): Development and Implementation. *J Med Internet Res.* 2021;23(7):e27633.

doi: 10.2196/27633

29. D'Angelo A, Kilili H, Chapman R, *et al.* Immune-related pan-cancer gene expression signatures of patient survival revealed by NanoString-based analyses. *PLoS ONE.* 2023;18(1):e0280364.

doi: 10.1371/journal.pone.0280364

30. Turan T, Kongpachith S, Halliwill, K, *et al.* A balance score between immune stimulatory and suppressive microenvironments identifies mediators of tumour immunity and predicts pan-cancer survival. *Br J Cancer* 2021;124(4):760–769.

doi: 10.1038/s41416-020-01145-4

31. Anderson AC, Joller N, Kuchroo VK. Lag-3, Tim-3, and TIGIT: Co-inhibitory Receptors with Specialized Functions in Immune Regulation. *Immunity*. 2016;44(5):989–1004.

doi: 10.1016/j.immuni.2016.05.001

32. Yang ZZ, Kim HJ, Wu H, *et al.* TIGIT Expression Is Associated with T-cell Suppression and Exhaustion and Predicts Clinical Outcome and Anti-PD-1 Response in Follicular Lymphoma. *Clin Cancer Res.* 2020;26(19):5217–5231.

doi: 10.1158/1078-0432.CCR-20-0558

33. Aliazis K, Christofides A, Shah R, *et al.* The tumor microenvironment's role in the response to immune checkpoint blockade. *Nature Cancer*. 2025;6(6):924–937.

doi: 10.1038/s43018-025-00986-3

34. Danaher P, Warren S, Lu R, *et al.* Pan-cancer adaptive immune resistance as defined by the Tumor Inflammation Signature (TIS): results from The Cancer Genome Atlas (TCGA). *J Immunother Cancer* 2018;6(1):63.

doi: 10.1186/s40425-018-0367-1

35. Wherry EJ, Kurachi M. Molecular and cellular insights into T cell exhaustion. *Nature reviews. Immunology*. 2015;15(8):486–499.

doi: 10.1038/nri3862

36. Blank CU, Haining WN, Held W, *et al.* Defining 'T cell exhaustion.' *Nat Rev Immunol*. 2019;19(11):665-674.

doi: 10.1038/s41577-019-0221-9

37. Jiang Y, Li Y, Zhu B. T-cell exhaustion in the tumor microenvironment. *Cell Death Dis.* 2015;6(6):e1792.

doi: 10.1038/cddis.2015.162

38. Joller N, Kuchroo VK. Tim-3, Lag-3, and TIGIT. *Curr Top Microbiol Immunol.* 2017;410:127–156.

doi: 10.1007/82_2017_62

39. Venkatachalapathy M. Targeting intratumoral Tregs: The promise of CD25×TIGIT bispecific antibodies in solid tumor therapy. *Mol Ther.* 2024;32(11):3758–3760.

doi: 10.1016/j.ymthe.2024.10.013

40. Ge Z, Zhou G, Campos Carrascosa L, *et al.* TIGIT and PD1 Co-blockade Restores ex vivo Functions of Human Tumor-Infiltrating $CD8^+$ T Cells in Hepatocellular Carcinoma. *Cell Mol Gastroenterol Hepatol.* 2021;12(2):443–464.

doi: 10.1016/j.jcmgh.2021.03.003

41. Zhou L, Velegraki M, Wang Y, *et al.* Spatial and functional targeting of intratumoral Tregs reverses CD8+ T cell exhaustion and promotes cancer immunotherapy. *J Clin Investig.* 2024;134(14):e180080.

doi: 10.1172/JCI180080

42. Nutsch K, Banta KL, Wu TD, *et al.* TIGIT and PD-L1 co-blockade promotes clonal expansion of multipotent, non-exhausted antitumor T cells by facilitating co-stimulation. *Nature Cancer*. 2024;5(12):1834–1851.

doi: 10.1038/s43018-024-00870-6

43. Ma J, Yan S, Zhao Y, *et al.* Blockade of PD-1 and LAG-3 expression on CD8+ T cells promotes the tumoricidal effects of CD8+ T cells. *Front Immunol.* 2023;14:1265255.

doi: 10.3389/fimmu.2023.1265255

44. Zheng S, Wang W, Shen L, Yao Y, Xia W, Ni C. Tumor battlefield within inflamed, excluded or desert immune phenotypes: the mechanisms and strategies. *Exp Hematol Oncol.* 2024;13(1):80.

doi: 10.1186/s40164-024-00543-1

45. Tiwari A, Oravecz T, Dillon LA, *et al.* Towards a consensus definition of immune exclusion in cancer. *Front Immunol.* 2023;14:1084887.

doi: 10.3389/fimmu.2023.1084887

46. Kather JN, Suarez-Carmona M, Charoentong P, *et al.* Topography of cancer-associated immune cells in human solid tumors. *eLife*. 2018;7:e36967.

doi: 10.7554/eLife.36967

47. Chen DS, Mellman I. Elements of cancer immunity and the cancer-immune set point. *Nature*. 2017;541(7637):321–330.

doi: 10.1038/nature21349

48. Lindskrog SV, Prip F, Lamy P, *et al.* An integrated multi-omics analysis identifies prognostic molecular subtypes of non-muscle-invasive bladder cancer. *Nature Commun.* 2021;12(1):2301.

doi: 10.1038/s41467-021-22465-w

49. Mezheyeuski A, Backman M, Mattsson J, *et al.* An immune score reflecting pro- and anti-tumoural balance of tumour microenvironment has major prognostic impact and predicts immunotherapy response in solid cancers. *eBioMedicine*. 2023;88:104452.

doi: 10.1016/j.ebiom.2023.104452

50. Yang X, Luo B, Tian J, *et al.* Biomarkers and ImmuneScores in lung cancer: predictive insights for immunotherapy and combination treatment strategies. *Biol Proced Online.* 2025;*27*(1):25.

doi: 10.1186/s12575-025-00287-0

51. Teng F, Meng X, Wang X, *et al.* Expressions of CD8+TILs, PD-L1 and Foxp3+TILs in stage I NSCLC guiding adjuvant chemotherapy decisions. *Oncotarget*. 2016;7(39):64318–64329.

doi: 10.18632/oncotarget.11793

52. Simon S, Labarriere N. PD-1 expression on tumor-specific T cells: Friend or foe for immunotherapy? *Oncoimmunology*. 2017;7(1):e1364828.

doi: 10.1080/2162402X.2017.1364828

53. Que Y, Xiao W, Guan YX, *et al.* PD-L1 Expression Is Associated with FOXP3+ Regulatory T-Cell Infiltration of Soft Tissue Sarcoma and Poor Patient Prognosis. *J Cancer.* 2017;8(11):2018–2025.

doi: 10.7150/jca.18683

54. Damotte D, Warren S, Arrondeau J, *et al.* The tumor inflammation signature (TIS) is associated with anti-PD-1 treatment benefit in the CERTIM pan-cancer cohort. *J Transl Med.* 2019;17(1):357.

doi: 10.1186/s12967-019-2100-3

55. Sahin I, Turen S, Santapuram P, Sahin IH. The tumor microenvironment of pancreatic adenocarcinoma and immune checkpoint inhibitor resistance: a perplex relationship. *Cancer Drug Resist.* 2020;3(4):699–709.

doi: 10.20517/cdr.2020.48

56. Finan JM, Guo Y, Goodyear SM, Brody J.R. Challenges and Opportunities in Targeting the Complex Pancreatic Tumor Microenvironment. *JCO Oncol Adv.* 2024;1:e2400050.

doi: 10.1200/OA-24-00050

57. Lindau D, Gielen P, Kroesen M, Wesseling P, Adema GJ. The immunosuppressive tumour network: myeloid-derived suppressor cells, regulatory T cells and natural killer T cells. *Immunology*. 2013;138(2):105–115.

doi: 10.1111/imm.12036

58. Haist M, Stege H, Grabbe S, Bros M. The Functional Crosstalk between Myeloid-Derived Suppressor Cells and Regulatory T Cells within the Immunosuppressive Tumor Microenvironment. *Cancers*. 2021;13(2):210.

doi: 10.3390/cancers13020210

59. Tiwari JK, Negi S, Kashyap M, Nizamuddin S, Singh A, Khattri A. Pan-Cancer Analysis Shows Enrichment of Macrophages, Overexpression of Checkpoint Molecules, Inhibitory Cytokines, and Immune Exhaustion Signatures in EMT-High Tumors. *Front Oncol.* 2022;11:793881.

doi: 10.3389/fonc.2021.793881

60. Nadjafikhah M, Nasiri M. A comparative study of manifold learning methods for scRNA-seq with a trajectory-aware metric. *Sci Rep*. 2025;15(1):28923.

doi: 10.1038/s41598-025-14301-8

61. Li W, Cerise JE, Yang Y, Han H. Application of t-SNE to human genetic data. *J Bioinform Comput Biol.* 2017;15(04):1750017.

doi: 10.1142/S0219720017500172

62. Cieslak MC, Castelfranco AM, Roncalli V, Lenz PH, Hartline D.K. t-Distributed Stochastic Neighbor Embedding (t-SNE): A tool for eco-physiological transcriptomic analysis. *Mar Genom.* 2020;51:100723.

doi: 10.1016/j.margen.2019.100723

63. Silva R, Melo-Pinto P. t-SNE: A study on reducing the dimensionality of hyperspectral data for the regression problem of estimating oenological parameters. *Artif Intell Agric.* 2023;7:58–68.

doi: 10.1016/j.aiia.2023.02.003